

# Evolution of the Kondo Effect in a Quantum Dot Probed by the Shot Noise

Yoshiaki Yamauchi<sup>1</sup>, Koji Sekiguchi<sup>1</sup>, Kensaku Chida<sup>1</sup>, Tomonori Arakawa<sup>1</sup>, Shuji Nakamura<sup>1</sup>, Kensuke Kobayashi<sup>1\*</sup> and Teruo Ono<sup>1</sup>, Tatsuya Fujii<sup>2</sup>, Rui Sakano<sup>3</sup>

<sup>1</sup>*Institute for Chemical Research, Kyoto University, Uji, Kyoto 611-0011, Japan.*

<sup>2</sup>*Institute for Solid State Physics, University of Tokyo, Kashiwa, Chiba 277-8581, Japan. and*

<sup>3</sup>*Department of Applied Physics, University of Tokyo, Hongo, Tokyo 113-0033, Japan.*

(Dated: July 10, 2018)

We measure the current and shot noise in a quantum dot in the Kondo regime to address the nonequilibrium properties of the Kondo effect. By systematically tuning the temperature and gate voltages to define the level positions in the quantum dot, we observe an enhancement of the shot noise as temperature decreases below the Kondo temperature, which indicates that the two-particle scattering process grows as the Kondo state evolves. Below the Kondo temperature, the Fano factor defined at finite temperature is found to exceed the expected value of unity from the noninteracting model, reaching  $1.8 \pm 0.2$ .

PACS numbers: 72.15.Qm, 72.70.+m, 73.23.-b, 73.23.Hk

As the Kondo effect is one of the most fundamental many-body phenomena in condensed matter physics [1], its realization in a quantum dot (QD) [2] would be an attractive stage at which various theoretical predictions for Kondo physics can be tested in a way otherwise impossible. Indeed, the dependence of this effect on several external parameters such as temperature, bare level position, and magnetic field has been precisely compared with theory [2, 3]. Many other aspects of the Kondo state, such as its coherence [3–5], have been tested, which has deepened our understanding of how a local spin interacts with continuum to form a correlated ground state.

Most of the experiments performed thus far using a Kondo QD have focused on the equilibrium properties of the Kondo effect; however, it is also possible to investigate the nonequilibrium correlated states (for example, see Refs. [6, 7]). An experiment on the shot noise or the nonequilibrium fluctuation in the current [8] passing through a Kondo QD [9, 10] would be valuable as it would yield quantitative values for comparison with existing theories [11–18]. Several theories predict that shot noise in a Kondo QD is enhanced by two-particle scattering with a Fano factor larger than that expected in a noninteracting case. A pioneering experiment was performed to tackle this problem [9]; however, the versatile controllability of a Kondo QD and the universality of Kondo physics have still not been investigated in detail.

Here, we report an experiment for the measurement of current and shot noise through a Kondo QD. Upon systematic tuning of the temperature and gate voltages, we observed an enhancement of the shot noise in the QD with a decrease in the temperature to below the Kondo temperature, which indicates the evolution of the nonequilibrium Kondo state. We discuss this observation in terms of the finite-temperature Fano factor [15–17, 19], which, well below the Kondo temperature, exceeds the expected value of unity from the noninteracting model.

The experiment was performed on a QD fabricated

on GaAs/AlGaAs two-dimensional electron gas (electron mobility of  $2.7 \times 10^5$  cm<sup>2</sup>/Vs and electron density of  $2.4 \times 10^{11}$  cm<sup>-2</sup> at 4.2 K) with four Au/Ti metallic gate electrodes patterned by electron beam lithography. A scanning electron microscopy (SEM) image of the QD and a schematic of the experimental setup for measuring the current and noise in the dilution refrigerator are shown in Fig. 1(a).

The noise was measured as follows [20–22]. The voltage fluctuation  $S_v$  across the sample on the resonant ( $LC$ ) circuit, whose resonance frequency was set to 2.65 MHz with a bandwidth of  $\sim 140$  kHz, was extracted as an output signal of the cryogenic amplifier followed by a room-temperature amplifier. The time-domain signal was captured by a digitizer and converted to spectral density via fast-Fourier transform. Fitting of the resonance peak gave  $S_v$ . To derive the current noise power spectral density  $S_i$  of the sample, the noise measurement setup had to be calibrated. As the cryogenic amplifier has finite voltage and current noises ( $S_v^{amp}$  and  $S_i^{amp}$  in terms of the amplifier input), the measured  $S_v$  for the sample with resistance  $R$  is related to  $S_i$  as  $S_v = A (S_v^{amp} + 1/(1/R + 1/Z)^2 (S_i^{amp} + S_i))$ . Here,  $A$  and  $Z$  are the gain of the amplifiers and the impedance of the  $LC$  circuit at the resonance frequency, respectively. To extract these parameters, the thermal noise  $S_i = 4k_B T/R$  (where  $k_B$  is the Boltzmann constant) was measured for about 30 different  $R$ 's between 10 k $\Omega$  and 70 k $\Omega$  at eight different temperatures ( $T$ ) below 800 mK. We obtained  $A = 1.1 \times 10^6$  V<sup>2</sup>/V<sup>2</sup>,  $Z = 72$  k $\Omega$ ,  $S_v^{amp} = 8.4 \times 10^{-20}$  V<sup>2</sup>/Hz, and  $S_i^{amp} = 1.9 \times 10^{-28}$  A<sup>2</sup>/Hz. To derive the current noise at the QD ( $S_I$ ) from  $S_i$ , the thermal noise of the contact resistance was taken into account. We confirmed that the electron (noise) temperature  $T$  can be controlled to be between 130 mK and 800 mK. The estimated resolution of  $S_I$  of the present setup was  $2 \times 10^{-29}$  A<sup>2</sup>/Hz.

Upon tuning the voltages of the four gate electrodes

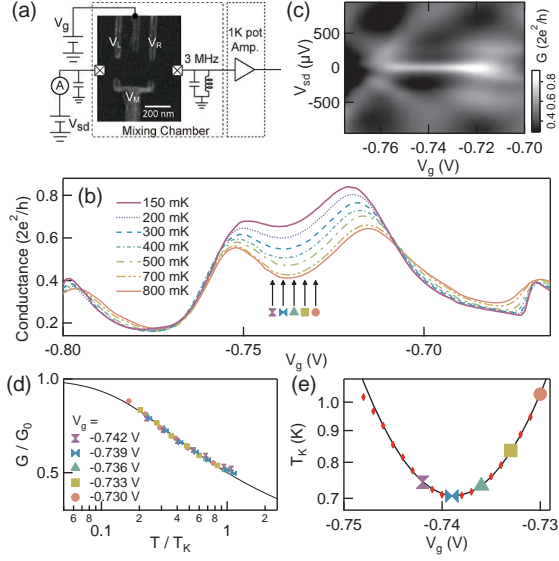


FIG. 1. (a) SEM image of a QD in the current and noise measurement setup in a dilution refrigerator. The negative voltages  $V_g$ ,  $V_L$ ,  $V_R$ , and  $V_M$  are applied to the gates to define the QD. (b) Conductance as a function of  $V_g$  at various temperatures between 150 mK and 800 mK. The positions for  $V_g = -0.742$ ,  $-0.739$ ,  $-0.736$ ,  $-0.733$ , and  $-0.730$  V are indicated by special marks (see (d) and (e)). (c) Coulomb diamond at 150 mK with a Kondo resonance at around  $V_g \sim -0.74$  V. (d) Scaling plot of conductance as a function of  $T$ . (e) Gate voltage dependence of  $T_K$ . The curve represents the expected  $T_K$  for  $U = 0.56$  meV and  $\Gamma = 0.34$  meV.

( $V_g$ ,  $V_L$ ,  $V_R$ , and  $V_M$  shown in Fig. 1(a)), the conductance  $G$  through the QD showed typical behavior expected for the Kondo effect. Further, as shown in Fig. 1(b), upon decreasing  $T$  from 800 mK to 150 mK, the conductance at the Coulomb valley centered around  $V_g \sim -0.74$  V enhanced, whereas conductance in the neighboring valleys around  $V_g \sim -0.77$  V and  $-0.68$  V did not show enhancement. This indicates that the number of electrons is odd at the valley around  $V_g \sim -0.74$  V and the Kondo effect appears at low temperatures [2]. In fact, the differential conductance at finite source-drain voltages ( $V_{sd}$ ) at  $T = 150$  mK shows a peak structure, namely, Kondo resonance, between  $V_g = -0.71$  V and  $-0.75$  V as shown in Fig. 1(c).

To quantitatively discuss the Kondo effect in a QD, it is important to derive several basic parameters to characterize it. To this end, we adopted a previously reported method [3, 5, 7, 23]. First, we numerically fit the temperature dependence of the conductance at a given  $V_g$  to derive the  $V_g$ -dependent Kondo temperature ( $T_K$ ), as  $V_g$  modulates the bare level position and hence  $T_K$ . We used the empirical function  $G(T) = G_0/(1 + (2^{1/s} - 1)(T/T_K)^2)^s$ , where  $s \approx 0.2$  for a spin-1/2 Kondo system. By taking  $s = 0.18$  and  $G_0 = 0.83G_q$  ( $G_q \equiv 2e^2/h \sim (12.9 \text{ k}\Omega)^{-1}$ ), we adequately scaled the

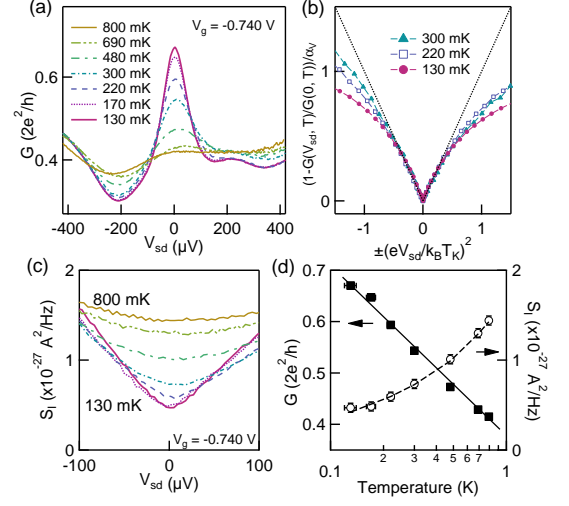


FIG. 2. (a) Differential conductance  $G(V_{sd}, T)$  at  $V_g = -0.740$  V for several temperatures between 130 mK and 800 mK. (b) Plot of  $(1 - G(V_{sd}, T)/G(0, T))/\alpha_V$  versus  $(eV_{sd}/k_B T_K)^2$  [7]. The solid line shows the associated universal curve. (c) Current noise spectral density  $S_I(V_{sd})$  corresponding to  $G(V_{sd})$  shown in (a). (d) Temperature dependence of zero-bias conductance and thermal noise at  $V_g = -0.740$  V.

temperature dependence of the conductance as shown in Fig. 1(d), where the normalized conductance  $G/G_0$  is plotted against the normalized temperature  $T/T_K$ . As the two barriers for defining the QD are asymmetric [23],  $G_0/G_q$  is less than unity. The obtained  $T_K$ 's are plotted as a function of  $V_g$  in Fig. 1(e).  $T_K$  was determined by the charging energy ( $U$ ), the energy level of the single-particle state ( $\epsilon_0$ ), and its width ( $\Gamma$ ) as  $T_K = \sqrt{\Gamma U}/2 \exp((\pi\epsilon_0(\epsilon_0 + U))/\Gamma U)$ . By numerical fitting,  $U$  and  $\Gamma$  were obtained as 0.56 meV and 0.34 meV, respectively. The obtained value of  $U$  is consistent with the Coulomb diamond shown in Fig. 1(c).

The differential conductance and current noise at  $V_g = -0.740$  V, which is close to the electron-hole symmetry point with the lowest  $T_K$  of 0.70 K, are shown in Figs. 2(a) and (c), respectively. Since  $\Gamma \gg k_B T_K$ , the low-energy properties are characterized by  $k_B T_K$ . The differential conductance  $G(T, V_{sd})$  at various  $T$  between 130 mK and 800 mK is shown in Fig. 2(a). As  $T$  decreases, a resonant peak emerges at zero bias voltage. Figure 2(b) shows the scaling plot of  $G(T, V_{sd})$ , where  $(1 - G(V_{sd}, T)/G(0, T))/\alpha_V$  is plotted as a function of  $(eV_{sd}/k_B T_K)^2$  with  $\alpha_V = c_T \alpha / (1 + c_T (\gamma/\alpha - 1)(T/T_K)^2)$  ( $e > 0$  is the electron charge). Here, we took  $\alpha = 0.10$ ,  $\gamma = 0.50$ , and  $c_T = \sqrt{2^{1/s}} - 1$  as reported before [7] and achieved good scaling of up to  $\sim 0.5(eV_{sd}/k_B T_K)^2$ , which supports the validity of the present analysis. Figure 2(d) shows the characteristic logarithmic enhancement of the conductance with decreasing temperature. Here, we superpose the equilibrium current noise (thermal noise) as

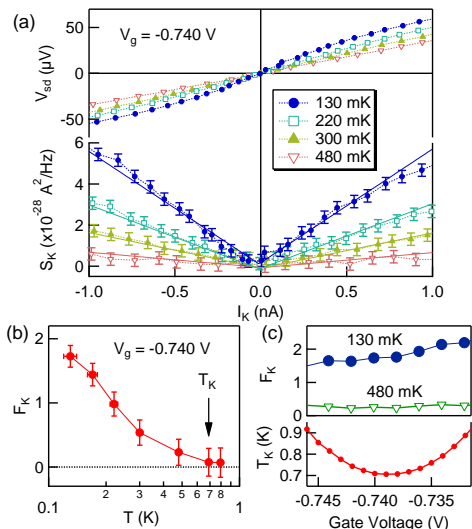


FIG. 3. (a) (upper) Relation between  $V_{sd}$  and  $I_K$  plotted for  $V_g = -0.740$  V and at various temperatures. (lower) Corresponding plot showing  $S_K$  as a function of  $I_K$ . The solid curves show the result of numerical fitting to obtain  $F_K$ . (b)  $F_K$  as a function of temperature. (c) Gate voltage dependence of  $F_K$  with  $T_K$  as a function of  $V_g$ .

a function of  $T$ , which is in good agreement with the Johnson-Nyquist relation  $S_I = 4k_B T G(V_{sd} = 0)$  represented by the dashed curve.

Based on the above properties of our Kondo QD, we analyzed the current noise  $S_I$  according to a recently proposed scheme [15–17, 19] in terms of the finite-temperature Fano factor for the Kondo system. The finite-temperature Fano factor  $F_K$  is defined as

$$F_K \equiv \frac{S_K}{2eI_K}, \quad (1)$$

where  $I_K$  and  $S_K$  are expressed using the observed current  $I(V_{sd}, T)$  and  $S_I(V_{sd}, T)$  as  $I_K \equiv I_0 - I(V_{sd}, T)$  and  $S_K \equiv S_I(V_{sd}, T) - 4k_B T G(V_{sd}, T) - S_0$ , respectively. Here,  $I_0 \equiv G_q(1 - \delta^2)V_{sd}$ , where  $\delta^2$  denotes the asymmetry of the two barriers of the QD. It should be noted that  $I_K$  is not the current back-scattered at the QD as was the case in Ref. [9], but is rather the deviation of the current from that at the Kondo fixed point. Similarly, at the fixed point, the asymmetry of the QD yields the corresponding shot noise contribution as expressed by  $S_0 \equiv 2eG_q\delta^2(1 - \delta^2)V_{sd}(\coth(x) - 1/x)$  with  $x \equiv eV_{sd}/2k_B T$ . In the absence of the Kondo correlation with  $U/\Gamma \rightarrow 0$ ,  $F_K = 1$ , which is in agreement with the noninteracting case [17, 18, 24].

Figure 3(a) shows the result of analysis of the current and shot noise obtained at  $V_g = -0.740$  V for 130, 220, 300, and 480 mK. The upper panel shows the relation between  $I_K$  and  $V_{sd}$ .  $I_K$  appears almost linear to  $V_{sd}$  at 480 mK, whereas nonlinearity becomes prominent as  $T$  decreases, reflecting the appearance of the Kondo effect.

The lower panel of Fig. 3(a) shows a plot of  $S_K$  against  $I_K$ . At any given  $I_K$ ,  $S_K$  increases with decreasing  $T$ . Remarkably,  $S_K$  is proportional to  $|I_K|$  for all temperatures and  $F_K$  can be determined by numerical fitting to Eq. (1). The obtained  $F_K$  is shown in Fig. 3(b) as a function of  $T$ . At  $T \gtrsim T_K = 0.70$  K,  $F_K = 0.1 \pm 0.3$ . As  $T$  decreases,  $F_K$  increases and reaches  $1.8 \pm 0.2$  at 130 mK. This suggests that  $F_K$  clearly indicates the evolution of the Kondo effect and that  $F_K > 1$  indicates the electron bunching due to Kondo correlation. This observation of the evolution of the nonequilibrium Kondo state as characterized by the growth of  $F_K$  with decreasing temperature is the main result of the present work.

Theoretically,  $F_K$  is predicted to be  $5/3$  [12–17], which is close to the value obtained here. In a realistic experimental situation, however,  $F_K$  may be smaller owing to several reasons. First, the asymmetry of the QD causes  $F_K$  to be smaller, i.e.,  $F_K = 5/3 - 8\delta^2/3$ , at  $T = 0$  [15]. Although no theoretical results are available for finite  $\delta^2$  at finite  $T$ ,  $F_K = 1.2$  is expected for  $\delta^2 = 1 - G_0/G_q = 0.17$  (present case) at  $T = 0$ . Second, the finite  $U/\Gamma$  also makes  $F_K$  smaller. In our case,  $F_K$  is predicted to be  $\sim 1.6$  instead of  $5/3$  [24]. Thirdly, finite temperature affects the estimation of  $F_K$  [15]; even for the symmetric case ( $\delta^2 = 0$ ), the value of  $5/3$  is reached only in a high bias region around  $eV_{sd}/k_B T \gg 10$  [15]. Thus, although the experimental value is in the same range as the theoretical one, the difference between them is not negligible as it indicates that there exists a mechanism for enhancing the shot noise of our QD in addition to the theoretical value. The reason for this is not yet understood. One possibility is that non-Kondo transport processes [7] such as inelastic cotunneling and/or finite transport through other levels in the QD contribute to the shot noise. For this finite transport process,  $U$  and  $\Gamma$  are of the same order in the present case; therefore, finite transport via the other adjacent levels, which are irrelevant to the Kondo state but are strongly coupled with the leads, might be possible. Even if the conductance of such transport is small, the backscattering due to it would cause an enhancement of the shot noise in the QD.

The above experimental result is reproducible in a wide parameter range for the single-particle level position. Figure 3(c) shows the obtained  $F_K$  with  $T_K$  as a function of  $V_g$ . The universality of Kondo physics predicts that  $F_K$  should be constant regardless of the level position at  $T \ll T_K$ ; however, in our case,  $F_K$  is found to be weakly dependent on  $V_g$  at 130 mK. This fact might support the aforementioned possible additional contribution to noise. At 480 mK,  $F_K$  becomes almost constant at a value less than unity. While  $T_K$  does not drastically vary as a function of  $V_g$ , the evolution of the Kondo effect is clearly visible in the case of a wide parameter range when  $T$  decreases below  $T_K$ .

Finally, the enhancement of the Fano factor is some-

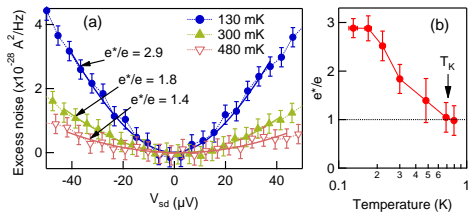


FIG. 4. (a) Excess current noise for  $V_g = -0.740$  V at 130 mK, 300 mK, and 480 mK as a function of  $V_{sd}$ . The solid curves are the result of fitting with the obtained  $e^*/e$  indicated. (b) Obtained  $e^*/e$  as a function of  $T$ .

times referred to as “effective charge” ( $e^*$ ) that is larger than  $e$ , although such  $e^*$  deduced by the measurement of shot noise in the Kondo regime should not be confused with an exotic charge like that in the fractional quantum Hall effect [12, 14–16]. In this sense, an analysis based on the Fano factor would be preferable to that based on  $e^*$ . Nevertheless, it is necessary to perform an “effective charge” analysis in order to compare our result with the experimental result that  $e^*/e \sim 5/3$ , which was in agreement with the theoretically predicted value [9]. In Fig. 4(a), the excess noise at  $V_g = -0.740$  V, where the contribution of thermal noise has been subtracted, is shown for 130, 300, and 480 mK. We fit these to  $S_I^{ex}(V_{sd}) = 2e^*V_{sd}G(1 - G/G_q)(\coth(x) - 1/x)$ , as was done before [9]. The bias window of this fitting is set to  $|eV_{sd}| \ll k_B T_K$ . As shown in Figs. 4(a) and 4(b),  $e^*/e = 2.9 \pm 0.2$  is obtained at 130 mK, whereas  $e^*/e$  is close to unity above  $T_K = 0.70$  K.  $e^*/e \sim 1$  was reported when the QD was tuned (by the gate voltage) to be outside the Kondo regime [9].

It is naively expected that  $e^*/e$  derived in this way equals  $F_K$  at  $T = 0$  [12, 13]. In the Kondo system at finite temperature, however, it is reasonable that  $F_K$  and  $e^*/e$  are different from each other, because the procedures for determining them are essentially different; the finite temperature that would affect the distance from the Kondo fixed point is taken into account in obtaining  $F_K$ . In contrast, to derive  $e^*/e$ , the system is treated as if it would obey noninteracting physics. The present  $e^*/e$  value of 2.9 at 130 mK is larger than the theoretical estimate of  $5/3$ . As discussed above,  $F_K$  (and hence  $e^*/e$  at  $T = 0$ ) is predicted to become smaller than  $5/3$  owing to several reasons. Therefore, both the present result and the value close to  $5/3$  reported in an asymmetric QD [9] support the suggestion that additional noise sources enhance the shot noise in the Kondo QD.

To conclude, we successfully observed the evolution of the Kondo state through the measurement of shot noise in a Kondo QD. With decreasing temperature, the Fano factor increases and exceeds the value in the noninteracting case, owing to two-particle scattering. The obtained

factors are larger than the theoretical factor, which may indicate that the shot noise in a Kondo QD is larger than the theoretical prediction. Further experimental effort, e.g., study of shot noise at the unitary limit in a perfectly symmetric QD, is necessary to quantitatively elucidate the nonequilibrium aspects of Kondo physics.

We are thankful to K. Kang, M. Hashisaka, S. Sasaki, and R. S. Deacon for fruitful discussions. This work was partially supported by KAKENHI and the Yamada Science Foundation.

\* kensuke@scl.kyoto-u.ac.jp

- [1] J. Kondo, Prog. Theor. Phys. **32**, 37 (1964).
- [2] D. Goldhaber-Gordon *et al.*, Nature **391**, 156 (1998); S. M. Cronenwett, T. H. Oosterkamp, and L. P. Kouwenhoven, Science **281**, 540 (1998); J. Schmid, J. Weis, K. Eberl, and K.v. Klitzing, Physica B **256-258**, 182 (1998).
- [3] W. G. van der Wiel *et al.*, Science **289**, 2105 (2000).
- [4] Y. Ji, M. Heiblum, D. Sprinzak, D. Mahalu, and H. Shtrikman, Science **290**, 779 (2000); Y. Ji, M. Heiblum, and H. Shtrikman, Phys. Rev. Lett. **88**, 076601 (2002).
- [5] M. Sato, H. Aikawa, K. Kobayashi, S. Katsumoto, and Y. Iye, Phys. Rev. Lett. **95**, 066801 (2005).
- [6] S. De Franceschi *et al.*, Phys. Rev. Lett. **89**, 156801 (2002); R. Leturcq *et al.*, *ibid.* **95**, 126603 (2005); J. Paaske *et al.*, Nature Phys. **2**, 460 (2006).
- [7] M. Grobis, I. G. Rau, R. M. Potok, H. Shtrikman, and D. Goldhaber-Gordon, Phys. Rev. Lett. **100**, 246601 (2008).
- [8] Y. M. Blanter and M. Büttiker, Phys. Rep. **336**, 1 (2000).
- [9] O. Zarchin, M. Zaffalon, M. Heiblum, D. Mahalu, and V. Umansky, Phys. Rev. B **77**, 241303(R) (2008).
- [10] T. Delattre *et al.*, Nature Phys. **5**, 208 (2009).
- [11] Y. Meir and A. Golub, Phys. Rev. Lett. **88**, 116802 (2002).
- [12] E. Sela, Y. Oreg, F. von Oppen, and J. Koch, Phys. Rev. Lett. **97**, 086601 (2006).
- [13] A. Golub, Phys. Rev. B **73**, 233310 (2006).
- [14] A. O. Gogolin and A. Komnik, Phys. Rev. Lett. **97**, 016602 (2006).
- [15] C. Mora, X. Leyronas, and N. Regnault, Phys. Rev. Lett. **100**, 036604 (2008); **102**, 139902(E) (2009); P. Vitushinsky, A. A. Clerk, and K. Le Hur, Phys. Rev. Lett. **100**, 036603 (2008).
- [16] C. Mora, P. Vitushinsky, X. Leyronas, A. A. Clerk, and K. Le Hur, Phys. Rev. B **80**, 155322 (2009).
- [17] T. Fujii, J. Phys. Soc. Jpn. **79**, 044714 (2010).
- [18] E. Sela and J. Malecki, Phys. Rev. B **80**, 233103 (2009).
- [19] T. Fujii, J. Phys. Soc. Jpn. **76**, 044709 (2007).
- [20] R. de-Picciotto *et al.*, Nature **389**, 162 (1997); M. Reznikov *et al.*, *ibid.* **399**, 238 (1999).
- [21] L. DiCarlo *et al.*, Rev. Sci. Instrum. **77**, 073906 (2006); M. Hashisaka *et al.*, *ibid.* **80**, 096105 (2009); M. Hashisaka *et al.*, J. Phys. Conf. Series **109**, 012013 (2008).
- [22] M. Hashisaka *et al.*, Phys. Rev. B **78**, 241303(R) (2008); S. Nakamura *et al.*, *ibid.* **79**, 201308(R) (2009).
- [23] D. Goldhaber-Gordon *et al.*, Phys. Rev. Lett. **81**, 5225 (1998).
- [24] R. Sakano, T. Fujii, and A. Oguri, Phys. Rev. B **83**, 075440 (2011).